Prospective Motion Correction via Real-Time Active Marker Tracking: An Image Quality Assessment

M. B. Ooi[1], S. Krueger[2], W. Thomas[3], and T. R. Brown[1,3]

[1]Department of Biomedical Engineering, Columbia University, New York City, New York, United States, [2]Philips Research, Hamburg, Germany, [3]Department of Radiology, Columbia University, New York City, New York, United States

Introduction: Subject motion is a fundamental problem in MRI. Movement of the tissue being imaged during the acquisition of MR data causes image artifacts due to erroneous positional encoding of the k-space data, manifesting in image-space as blurring or ghosting. Often, it is subject populations with the most to benefit – young children, elderly subjects, and patients with dementia – where the utility of MRI is curtailed by motion artifact. Even amongst a healthy elderly population, our experience suggests that significant motion artifacts may appear in 30% of images, with 10-20% showing relatively severe motion. These difficulties underline the importance of an effective motion correction strategy. Several comparable prospective motion tracking strategies have been presented in literature – including PACE [1], 3D spherical navigators [2,3], and optical tracking [4] – each with their own advantages and disadvantages. We believe the proposed use of active markers for prospective motion correction to be a more-than-competitive solution to the problem of head-motion.

Active marker tracking using micro RF-coils was introduced by [5], and first used for motion correction in an inter-image update scheme [6]. Recently, this has been extended into a real-time, intra-image motion compensation package, where qualitative improvements in human brain images were presented [7]. This current work follows up on this latest development by further investigating, with quantitative metrics, the improvements in image quality allowed by this technique.

Methods: Experiments were performed on a 1.5T Philips Achieva (Philips Medical Systems, Best, The Netherlands). The 32-channel MR system allows for parallel imaging with any SENSE-coil (SENSitivity Encoding), and position tracking via our custom three tracking-coil apparatus (*Figure 1*). The tracking-coils were interfaced to the scanner via Synergy Multi-Connect (SMC) Box. Three of the channels were designated to receive the tracking coil signals, allowing a plane to be uniquely tracked in 3D-space.

Our motion correction software algorithm was implemented in Philips Pulse Programming Environment (PPE) R2.1.3. The tracking pulse-sequence consists of sequential gradient-echo readouts in each of the three orthogonal gradient directions; in this manner the position of each active marker can be uniquely determined in 3D-space, with a reported relative accuracy of <100μm [7]. At the beginning of the exam, the tracking-sequence is performed and initial reference tracking-coil locations are determined. The tracking-sequence is then interleaved into the following imaging pulse-sequence at a variable rate depending on the amount of motion present. At the next tracking shot, the active-marker locations are again determined, and compared with the initial reference locations; the rotation matrix and translation vector necessary for rigid-body realignment of these points is calculated [8], and the necessary imaging-plane geometry updated for motion correction. This iteration of tracking and imaging continues until all of the desired k-space – with corrected geometry independent of motion – is acquired; the total time for tracking, calculations, and geometry updates is ~ 20ms per tracking iteration. In cases of extreme/abrupt motion, a rejection strategy is executed where potentially corrupted lines of k-space are rejected and reacquired with the updated geometry. [7]

FIG. 1:

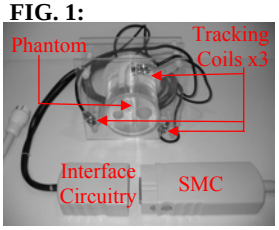

This initial validation study was chosen to be performed on phantoms for their well-defined geometry and clean edges – to facilitate the subsequent frequency domain and edge analysis – and better reproducibility of the controlled motions to be tested. Four reproducible experimental conditions were investigated: no motion, 10º, 20º, and 30º of abrupt through-plane rotation mid-scan. For each motion range, two image volumes were acquired – one with the motion-correction package ON, and one OFF – resulting in 8 image sets for analysis. A 3D-TFE sequence (TR = 6.3ms, TE = 1.97ms, θ = 40º, TFE-factor = 50, FOV = 300x300x25mm, matrix = 640, SENSE-cardiac coil) was used for imaging, allowing the investigation of motion effects on a 3D-volume as corruption in any part of the 3D k-space acquisition will affect the entire reconstructed image.

FIG. 2:

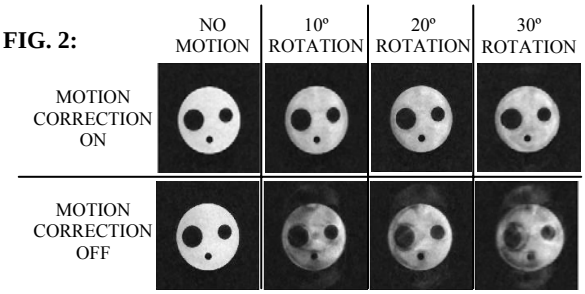

To assess improvements in image quality during acquisition in the presence of motion, two metrics are investigated: power spectrum analysis at low frequencies (homogeneous regions) and high frequencies (edges), and edge drop-off between contrast-boundaries. Power spectra over the entire imaging volume were generated (Mathworks, Natick, MA, USA). A cutoff frequency ω_C = 0.3 cycles/cm was chosen as the delineation between edged vs. smooth image characteristics; power spectrum below ω_C was integrated to yield total low-frequency power in the volume, and power spectrum above ω_C integrated for the volume's total high-frequency power (both are represented as a percentage by normalizing to the volume's total power over all frequencies). In order to minimize high frequency noise contributions in the subsequent frequency domain analysis, images were preprocessed with a median filter (width = 7).

FIG. 3:

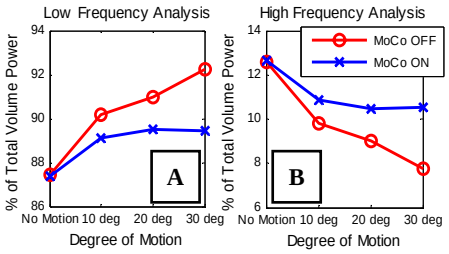

Results: As amount of induced motion increases (*Figure 2*), blurring in the uncorrected images increases, while the edge definition in the motion-corrected phantoms remains consistent. This is reflected quantitatively in the power spectrum analysis (*Figure 3*). The percentage of total power contributed by high k-space frequencies (*Figure 3(b)*) – corresponding to edges in image-space – within the volume of motion-compensated images remains fairly constant, suggesting that most of the edge definition within the volume has been preserved. In contrast, for uncompensated acquisitions, high frequency power decreases as degree of motion increases, reflecting the blurring and loss of edge quality we see in *Figure 2*. The same effect is mirrored at low frequencies (*Figure 3(a)*), showing the redistribution of image power from edges to blurring in uncompensated images.

FIG. 4:

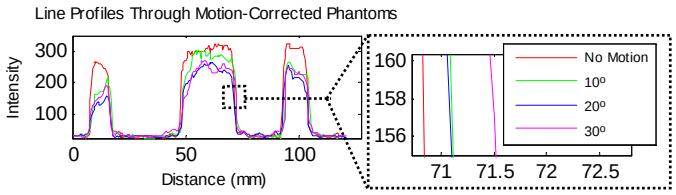

Our second metric (*Figure 4*) shows us in image-space the quality of the edge sharpness reflected in metric one. The line profiles are drawn across the "eyes" of each phantom. Over all the motion tested, the edge dispersion is within 0.7mm at FWHM, and for the 10º, 20º rotations it is within the in-plane resolution (0.47mm) of the acquisition. At the same edge, line profiles of the uncorrected phantoms (not shown) vary by up to 5mm – demonstrating a dramatic improvement with this motion correction strategy. Differences in profiles may be attributed to B0, B1 inhomogeneities, and low SNR is partly the result of distance between the imaging coil and phantom in the current setup.

Conclusion & Future Direction: The experimental results validate the potential benefits of the presented motion correction strategy by demonstrating quantitative improvements in image quality, adding additional evidence in support of the initial feasibility study [7]. Future investigation will include optimizing the trade-off between tracking frequency and added scan time, and determining the upper limits of motion (magnitude, direction, velocity, periodicity, etc.) that can be acceptably compensated for; these goals will require more rigorous quantitative testing in both phantom and human. Utility in other MR applications other than structural imaging, for example EPI pulse-sequences in fMRI/ASL and the effects of the tracking RF on spin-history, are also potential avenues of exploration.

References: [1] Thesen S et al., MRM, 44(3): 457-65, 2000. [2] Welch EB et al., MRM, 47(1): 32-41, 2002. [3] Ari N et al., Proc 14th ISMRM, 3195, 2006. [4] Zaitsev M et al., NEUROIMAGE, 31 (3): 1038-1050, 2006. [5] Dumoulin CL et al., MRM, 29(3): 411-5, 1993. [6] Derbyshire JA et al., JMRI, 8(4): 924-32, 1998. [7] Krueger S et al., Proc 14th ISMRM, 3196, 2006. [8] Umeyama S, IEEE Trans PAMI, 13(4): 376-380, 1991.